DOI: 10.1002/chem.200601123

The Preferred Reaction Path for the Oxidation of Methanol by PQQ-Containing Methanol Dehydrogenase: Addition–Elimination versus Hydride-Transfer Mechanism

Monica Leopoldini, Nino Russo,* and Marirosa Toscano[a]

Abstract: The catalytic oxidation of methanol to formaldehyde by pyrroloquinoline quinone (PQQ)-containing methanol dehydrogenase (MDH) was investigated at density functional B3LYP level. The still controversial addition–elimination and hydride-transfer reaction mechanisms were analysed. Computations performed in the gas phase and in the protein environment indicated that both suggested reaction sequences involve very high activation barriers. In this situation, the reactions should have scarce probability to occur and the preference for one of the two paths cannot be stated. Here, we will show how some corrections to the successive steps in the addition–elimination mechanism can sensibly decrease the activation barriers height, making possible the determination of the MDH-preferred catalytic path.

Keywords: density functional calculations · enzyme catalysis · methanol · oxidation · reaction mechanisms

Introduction

Quinoproteins constitute a class of dehydrogenase enzymes that convert alcohols and amines to the corresponding aldehydes and lactones.[1] The catalytic mechanism of these enzymes involves the quinone containing prosthetic groups. Cofactors are the pyrroloquinoline quinone (PQQ), the tryptophan tryptophyl quinone (TTQ)[2,3] (derived from two tryptophan residues), the topa-quinone (TPQ),[4,5] and the lysyl tyrosylquinone (LTQ).[6]

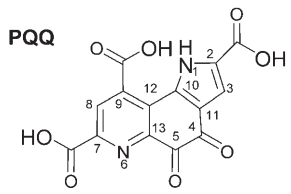

The PQQ-containing enzymes subclass, of which the methanol dehydrogenase (MDH)[7–9] and the glucose dehydrogenase (GDH)[10] are the main representatives, is the best characterized but many aspects still remain unsolved.

Methanol dehydrogenase (EC number: 1.1.99.8) is found in the periplasm of methylotrophic and autotrophic bacteria[11–15] and plays a crucial role in the metabolism of these organisms. It catalyzes the oxidation of methanol (or other primary alcohols) to the corresponding aldehydes, with the release of two protons and two electrons.[16,17] Apart from the PQQ cofactor, MDH requires a divalent calcium cation for its catalytic activity.[12,18–20]

The X-ray structure of methanol dehydrogenase from the *Methylophilus methylotrophus* W3A1 (*M.* W3A1) organism was solved at 2.4 Å resolution.[21] The enzyme is a H_2L_2 heterotetramer in which molecular masses of the two subunits H and L are 62 and 8 kDa, respectively. Each heavy subunit contains a Ca^{2+} cation and a PQQ cofactor not covalently bound to the protein. The cofactor is located in a cavity near to the end of an A strand, and it is sandwiched between the indole ring of the residue Trp237 and the S–S bridge of the couple Cys103-Cys104.

The oxygen atoms of the PQQ are involved in several hydrogen bonds with the residues Glu55, Arg109, Thr153, Ser168, Arg324 and Asn387. The calcium ion is coordinated to the O_5, N_6 and $O_7\alpha$ atoms of PQQ, the $O_1\varepsilon$ and $O_2\varepsilon$ of Glu171, $O_1\delta$ of Asn255, and the $O_1\varepsilon$ of Asp297 (see Figure 1).[21]

Two mechanisms by which MDH oxidises methanol to formaldehyde were proposed (Scheme 1): the addition–elim-

[a] Dr. M. Leopoldini, Prof. N. Russo, Prof. M. Toscano
Dipartimento di Chimica and Centro di Calcolo
ad Alte Prestazioni per Elaborazioni
Parallele e Distribuite-Centro d'Eccellenza MIUR
Universita' della Calabria
87030 Arcavacata di Rende (CS) (Italy)
Fax: (+39) 0984-493390
E-mail: nrusso@unical.it

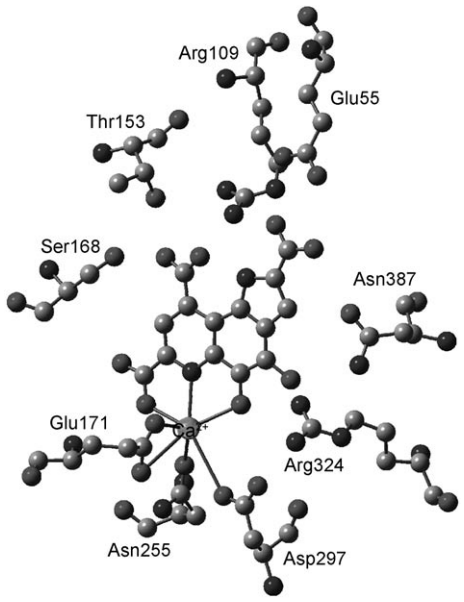

Figure 1. Methanol dehydrogenase active site.

ination (A)[8,22–24] and hydride transfer (B) mechanisms.[8,24,25]

Mechanism A involves the nucleophilic addition of the methanol oxygen to the PQQ carbonyl C_5, followed by the protonation of the cofactor and the H^+ abstraction from the substrate CH_3 by the PQQ oxygen attached to C_4, and the concomitant formation of a C_4–C_5 double bond in the PQQ, reduced to $PQQH_2$.

In mechanism B, a direct transfer of H^- to C_5 in the PQQ entails the direct formation of the product. The reduction of the cofactor to $PQQH_2$ is achieved through an internal enolization step.

For both processes, an acid–base catalysis takes place through the amino acid Asp297 that, for its location and chemical properties, may function as a base by abstracting the H^+ from the substrate hydroxyl and finally as an acid by donating the same proton to the cofactor.

Several experimental studies were devoted to the elucidation of the preferred reaction mechanism. Oubrie et al. obtained the crystal structure of soluble GDH[26] as a complex between the reduced $PQQH_2$ and glucose at 1.9 Å resolution in which the position of the C_1 atom in glucose was used to argue for a hydride-ion-transfer mechanism. Xia et al.[15,27,28] reported several crystal structures of MDH, postulating the hydride-transfer mechanism to be the preferred one. Molecular dynamics calculations[29] supported the hydride-transfer mechanism rather than the addition–elimination one. Recently, Kay and co-workers,[30] through electron paramagnetic resonance (EPR) studies on substrate binding to PQQ-Ca^{2+} in ethanol dehydrogenase, indicated a strong coordination of the substrate to the calcium cation which should be broken during the addition–elimination process. For this reason, mechanism A is unlikely. However, the experimental and theoretical information is not sufficient to clearly identify the catalytic mechanism followed by PQQ MDH and GDH enzymes.

With the purpose of highlighting the favoured catalytic mechanism of MDH among the previously proposed ones, a detailed theoretical investigation was carried out on metha-

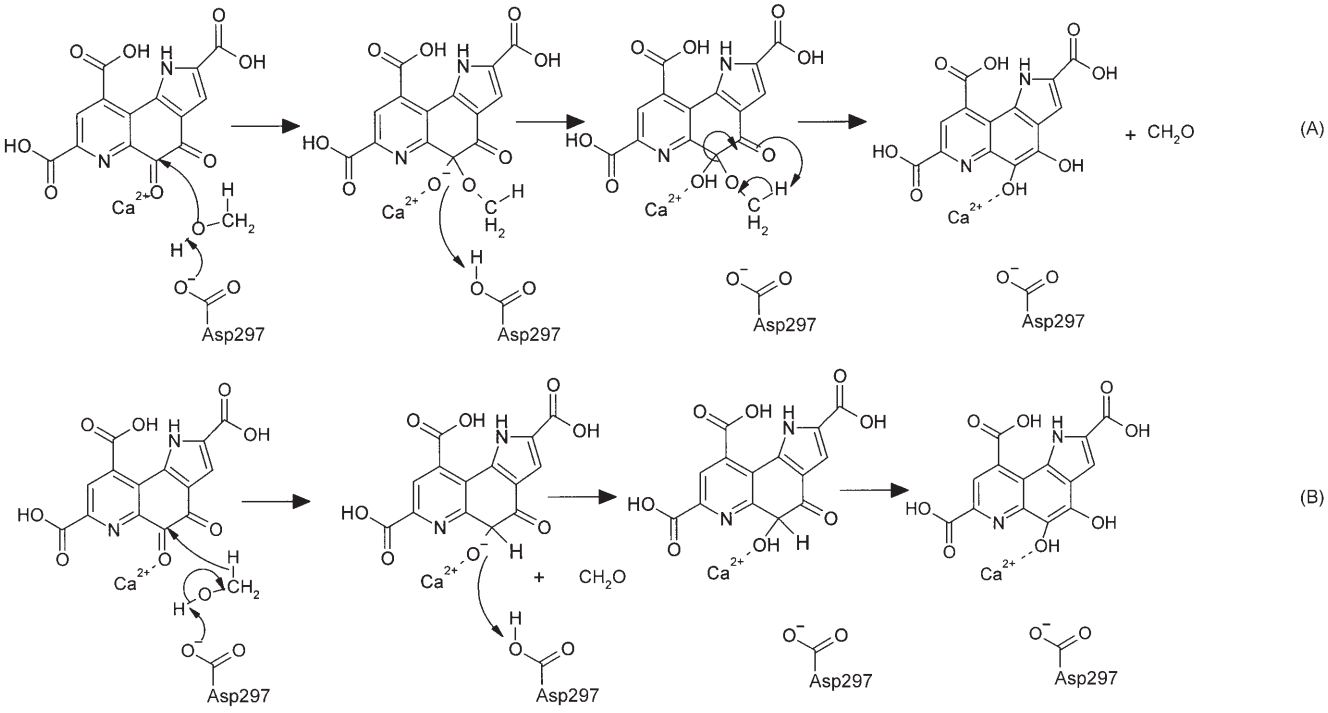

Scheme 1. Addition–elimination (A) and hydride-transfer (B) mechanisms proposed for the oxidation of methanol to formaldehyde by MDH.

nol oxidation by a MDH active-site model cluster. The employed model system, including the PQQ cofactor, Ca^{2+} coordinating groups and some nearby residues, allowed an extended analysis, which also included the role of the amino acids in the catalytic event.

Computational Details

All the computations reported here were carried out with the Gaussian 03 code,[31] employing the hybrid Becke exchange and Lee, Yang and Parr correlation (B3LYP)[32–35] functionals. The performance of the density functional B3LYP method in predicting properties of transition-metal-containing systems is satisfactory and supported by a large amount of literature papers concerning enzymatic catalysis.[36–47] The 6-31+G* basis set[48–51] was chosen for the C, N, O and H atoms, while for the calcium cation, the LANL2DZ pseudopotential in connection with the relative orbital basis set[52] was used.

Frequency calculations were performed at same level of theory on all stationary points of reaction paths with the aim of evaluating their character of minima or saddle points. Zero-point energy corrections, obtained from the vibrational analysis, were then included in all the relative energy values.

With the aim of confirming that a given transition state connects reactants and products, intrinsic reaction coordinate (IRC)[53,54] calculations were performed at the same level of theory.

Solvent effects were computed in the framework of self-consistent reaction field polarizable continuum model (SCRF-PCM)[55–57] in which the cavity is created by a series of overlapping spheres, by using the polarizable conductor calculation model (CPCM).[58,59] The universal force field (UFF) radii from the UFF force field[60] were used to build the cavity in the gas-phase equilibrium geometry. The dielectric constant value $\varepsilon = 4$ was chosen by taking into account the coupled effect of the protein itself and the water medium surrounding the protein, according to previous suggestions.[43–47] The relative solvent effects between minima and transition states are normally calculated to be quite small, within 2 kcal mol^{-1}.[43,44]

The active-site model cluster used in this work was constructed by starting from the X-ray structure of the protein from the microorganism *Methylophilus methylotrophus* W3A1 (PDB code = 1G72). The calcium cation first-shell coordination sphere consists of the PQQ molecule, two CH_3COO^- groups and a NH_3COCH_3 group which model the Glu171, Asn255 and Asp297 residues, respectively. To reproduce the hydrogen-bond network around the cofactor, two $(NH_2)_2CNHCH_3$ groups, a CH_3COO^- group, a NH_2COCH_3 group and a CH_3OH group were added as simplified models for the amino acids Glu55, Arg109, Ser168, Arg324 and Asn387. A hydrogen atom of each amino acidic residue was kept frozen at its crystallographic position to mimic the steric effects produced by the protein and to avoid an unrealistic expansion of the cluster during the optimization procedure. The substrate and product (CH_3OH and CH_2O) were left without constraints during the optimization.

Natural bond orbital (NBO) analysis[61] was carried out to determine net charges and some electronic properties.

Results and Discussion

Addition–elimination mechanism (A): The gas-phase potential-energy surface (PES) for the addition–elimination mechanism is reported in Figure 2a. The corresponding equilibrium geometries of the points belonging to path A (Scheme 1) are depicted in Figure 3.

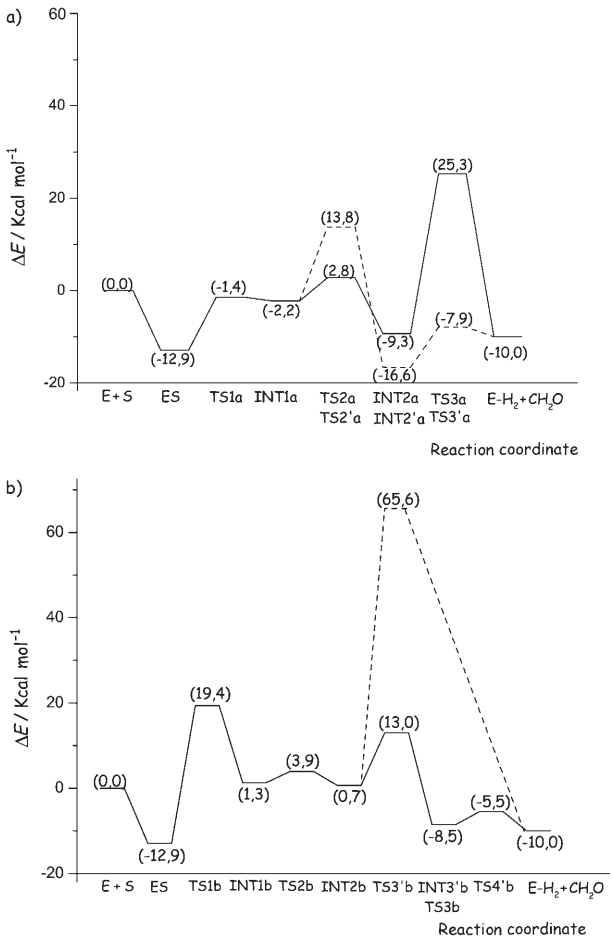

Figure 2. a) Gas-phase potential-energy surface for the addition–elimination and hydride transfer (b) mechanisms. The modified addition–elimination and the direct H^+ transfer for mechanisms A and B, respectively, are represented by -----. See text for details.

The starting point is represented by the formation of a Michaelis–Menten complex ES between the substrate and the catalytic centre, which is exothermic by 12.9 kcal mol^{-1}. The substrate interacts by its oxygen atom with the calcium cation, establishing a coordination bond of 2.51 Å. The substrate proton is involved in a hydrogen bond with the nega-

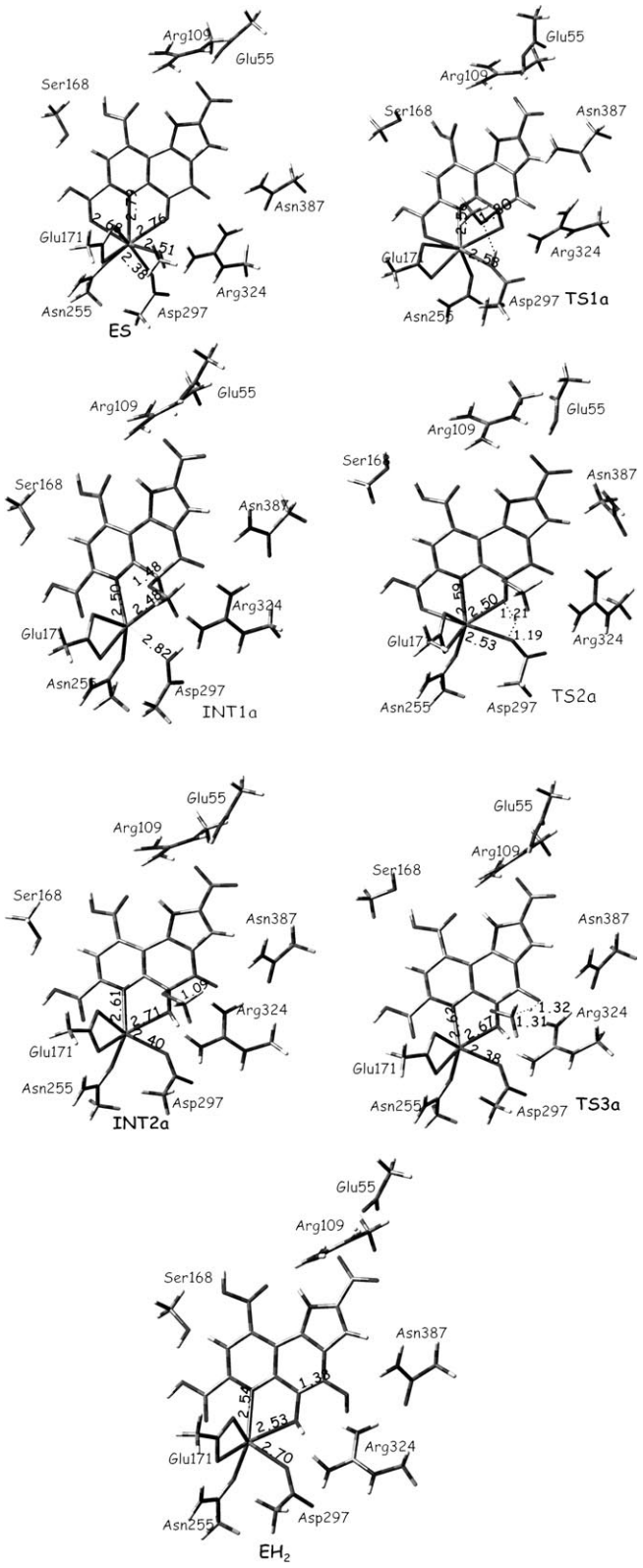

Figure 3. Optimized stationary points belonging to the addition–elimination path A.

tively charged oxygen of the Asp297 (1.90 Å). As a consequence, the Ca^{2+} ion interacts with the oxygen and nitrogen atoms of the PQQ (2.68, 2.76 and 2.79 Å, respectively), both the oxygen atoms of Glu171 (2.50 and 2.42 Å), the Asn255 carbonyl oxygen (2.41 Å), the $O_1\varepsilon$ of Asp297 (2.38 Å) and with the substrate oxygen. The coordination bond of the cofactor with the metallic centre contributes to the polarization of the PQQ C_5O carbonyl group. NBO analysis indicates that net charges on the C_5 and O atoms are 0.520 and -0.570 |e|, respectively. The positive charge of the calcium cation is reduced to 1.836 |e|.

Following the proposal for the addition–elimination, a saddle point for the nucleophilic addition of the substrate oxygen on the PQQ C_5 carbon atom is found (TS1a) at 1.4 kcal mol^{-1} below the reference (E+S). In TS1a, the formation of a O_{met}–C_5 bond, for which the critical distance is 1.80 Å (the subscript met refers to the methanol substrate), occurs in a concerted way with the shift of a proton from the alcoholic OH group to the $O_1\varepsilon$ atom of Asp297 which is coordinated to the cation. The normal vibration mode corresponds to the coupled stretchings of the incoming O_{met}–C_5 and H–$O_1\varepsilon$ bonds. However, the imaginary frequency of 160 cm^{-1} indicates that TS1a is mainly characterized by the motion of heavy atoms and that the potential energy surface for the transfer of the H^+ mediated by Asp297 is very flat. The PQQ C_5–O bond lengthens from 1.22 Å in the ES species up to 1.25 Å in TS1a. The activation energy is computed (with respect to the ES species) to be 11.5 kcal mol^{-1}.

The CH_3O^- addition to the PQQ leads to the tetrahedral intermediate INT1a in which the O_{met}–C_5 σ bond is completely formed (1.48 Å). The PQQ carbonyl oxygen attached to C_5 establishes a hydrogen bond with the NH_2 group of the Arg324 residue. The equilibrium structure of this species, which lies 2.2 kcal mol^{-1} below the reactants, suggests a hexacoordinated calcium cation because of a consistent weakening of the Ca^{2+}–O_{Asp} bond (2.82 Å in the INT1a versus 2.38 Å in the ES adduct).

The suggested literature mechanism provides for a proton transfer from HO-Asp to the PQQ C_5–O carbonyl oxygen which occurs through the transition-state TS2a. The proton is shared between the oxygen atoms of the PQQ (1.21 Å) and the Asp297 (1.19 Å) residue, respectively. The imaginary frequency at 1416 cm^{-1} refers to the stretching vibrational mode of the O_{Asp}–H and H–O_{PQQ} bonds. The geometrical features of this species are very similar to those of the INT1a intermediate (Figure 3). However, again the Asp297 oxygen atom moves closer to the metallic centre (Ca^{2+}–O_{Asp} distance is 2.53 Å). The energy required to overcome this TS2a is 5.0 kcal mol^{-1} as computed with respect to the INT1a intermediate (solid line).

The proton transfer leads to another intermediate along the reaction profile, INT2a, which is characterized by a calcium ion interacting with seven neighbouring N and O atoms. The CH_3 group of methanol approaches the PQQ oxygen atom attached to C_4 so that the latter is in a good position to favour the breaking of the H–CH_2 bond in the substrate (the distance H_{met}–O_{PQQ} is 2.72 Å). Gas-phase computations situate this species 9.3 kcal mol^{-1} below the reference (solid line).

The transition-state TS3a, which finally leads to the $PQQH_2$ reduced species, is found for C–H and H–O distance values of 1.31 and 1.32 Å, respectively. The bond between O_{met} and C_5 in the cofactor, lengthens up to 2.13 Å underling that it is going to break. The imaginary frequency at 1402 cm^{-1} corresponds to the movement of H^+ between the carbon and the oxygen atoms. The amount of energy of 34.6 kcal mol^{-1} required to overcome this barrier indicates that this step, responsible for the cleavage of the σ C–H bond in the substrate, is the rate-determining one.

The reaction products, that is, the reduced EH_2 species and CH_2O, are found 10.0 kcal mol^{-1} below the reference.

Hydride-transfer mechanism (B): In the second proposed mechanism (Scheme 1), the formation of the Michaelis–Menten complex ES is followed by a direct transfer of a hydride ion from the alcohol to the C_5 in the PQQ system. The H^- transfer should be concerted with the proton abstraction by the $O_1\varepsilon$ atom of the Asp297 residue, so that formaldehyde is immediately produced.

The optimized structures of the stationary points belonging to path B (Figure 2b) are reported in Figure 4.

The first transition-state TS1b that refers to the hydride addition, shows an imaginary frequency at 1413 cm^{-1} corresponding to the stretching of the bond between a substrate methyl hydrogen and the C_5 atom of PQQ coupled with the methanol deprotonation by Asp297. As in TS1 in path A, the potential-energy surface for the methanol deprotonation is very flat. The critical distances H_{met}–C_5 and H–CH_{2met} are 1.33 and 1.27 Å, respectively. TS1b requires an activation energy of 32.3 kcal mol^{-1}, as computed with respect to the ES. The cleavage of the covalent C–H bond in the methanol is energetically very expensive. The height of the barrier underlines that the hydride-transfer step is quite slow.

TS1b evolves into the INT1b intermediate lying at 1.3 kcal mol^{-1}, whereas the formaldehyde product already formed is leaving the active site. The C_5 carbon atom of INT1b changes its hybridization from sp^2 to sp^3 and establishes a covalent bond with the substrate hydrogen of 1.12 Å. The C_5O bond lengthens up to 1.37 Å.

The next step along the reaction profile, that is, the H^+ transfer from the Asp297 residue to the oxygen attached to C_5, occurs through transition-state TS2b which lies at 3.9 kcal mol^{-1}. The normal vibration mode at 1410 cm^{-1} corresponds to the shift of the proton from the Asp297 oxygen to the PQQ C_5O one. As can be seen from Figure 4, TS2b is a heptacoordinated species for which the geometrical parameters are very similar to those of the INT1b intermediate. This similarity explains the low activation barrier of 2.6 kcal mol^{-1} and the ease by which the H^+ transfer involving the Asp297 occurs.

The INT2b intermediate formed after the proton transfer is characterized by a tetrahedral C_5 carbon atom and by a network of hydrogen bonds that involve the PQQ oxygen atoms. C_4O carbonyl oxygen works as acceptor of the amino hydrogens present in Asn387 and Arg324 residues (2.48 and 1.90 Å, respectively). The newly formed hydroxyl linked to

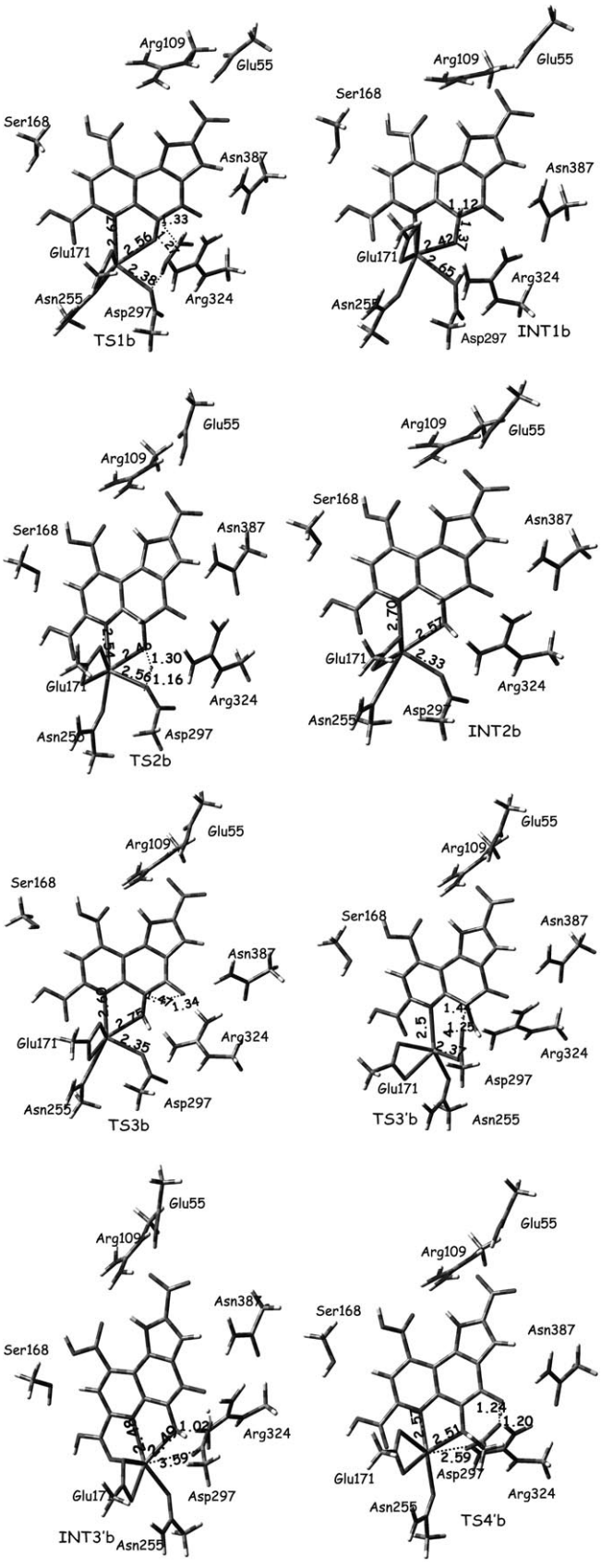

Figure 4. Optimized stationary points belonging to the hydride-transfer path B.

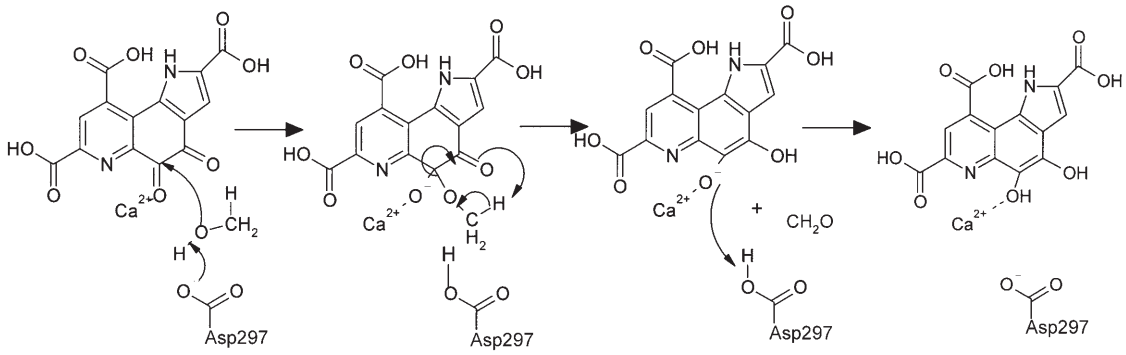

(C)

Scheme 2. Revised addition–elimination mechanism (C).

the C_5 atom establishes a hydrogen bond of 2.20 Å with the $-NH_2$ of Arg324.

The enolization process leading to the final reduced $PQQH_2$ cofactor occurs by transferring the hydrogen bound to C_5 to the C_4O carbonyl oxygen.

Transition-state TS3b for the direct hydrogen transfer on the C_4O oxygen atom is reached when the CH–O and C–HO critical distances assume the values of 1.34 and 1.47 Å, respectively. The imaginary frequency at 2260 cm^{-1} is assigned to the stretching of these bonds. TS3b is a highly stressed species, so that its formation, requiring 65.6 kcal mol^{-1}, is energetically prohibitive.

Alternately, the enolization process may be mediated by the Asp297 residue, emphasizing the role of this amino acid as a catalytic base. Two steps are necessary in this case: one that transfers the H^+ from the quinone to the $O_2\varepsilon$ of the aspartate, and another in which the protonation of the C_4O oxygen atom by the same residue occurs.

The transition state TS3′b, in which we can observe the incipient breaking and formation of C_5–H and $O_2\varepsilon$–H (in the Asp297) bonds, respectively, is characterized by an imaginary frequency of 1851 cm^{-1}. The proton appears to be shared between the two C_5 and $O_2\varepsilon$ atoms (C_5–H and $O_2\varepsilon$–H distances are 1.44 and 1.25 Å, respectively). In this species, the Asp297 rearranges itself in such a way to approach the aromatic ring of the cofactor. The heptacoordination around Ca^{2+} is retained in going from the INT2b intermediate to the TS3′b transition state. The energy required for this process is 12.3 kcal mol^{-1}.

From TS3′b, a stable intermediate INT3′b lying 8.5 kcal mol^{-1} below the reference originates. The Asp297 residue is now involved in two hydrogen bonds with the PQQ oxygen atoms. In the first bond, the hydroxyl attached to C_5 works as hydrogen donor (1.59 Å), in the second one, the C_4O carbonyl oxygen works as hydrogen acceptor (1.58 Å).

Through transition-state TS4′b, the second proton is transferred from the $O_2\varepsilon$ of Asp297 to the negatively charged oxygen atom attached to the C_4 atom of PQQ, finally leading to the $PQQH_2$ reduced species. The imaginary frequency at 1474 cm^{-1} refers to the stretching of the two $O_2\varepsilon$–H (1.20 Å) and C_4O–H (1.24 Å) bonds. The computed energetic expense to overcome this transition state is of 3.0 kcal mol^{-1}. A look to the paths in Figure 2 shows that the enolization may occur only if mediated by the aspartate residue.

Modified mechanism (C): As we have seen, the proposed mechanisms[8,22–24] A and B lead to two energetic profiles (Figure 2, solid lines) in which the final conversion of INT2a into the products through TS3a in the first path, and the hydride addition in the second one, are kinetically very slow; in particular, the reaction rates are not in the range of values expected for enzymatic catalysis. This fact puts us in doubt as to whether the suggested mechanisms represent the real ones. Thus, we have revised the literature proposal, paying particular attention to the addition–elimination process in which we have foreseen some possibility of improvement. The new reaction sequence is depicted in Scheme 2.

The optimized structures of the stationary points belonging to the new reaction profile (traced in Figure 2a with a dashed line) are depicted in Figure 5.

In this mechanism, (C), we propose that the proton shift from the aspartate residue to the PQQ oxygen atom belonging to the C_5O carbonyl group (TS2a) can occur after the substrate C–H bond cleavage. However, no experimental evidence can thwart this hypothesis.

If we assume the protonation of the cofactor as the last step, the obtained PES becomes quite different with respect to before (dashed line in Figure 2a). Starting from the INT1a intermediate, the transition state (TS2′a) describing the C–H bond breaking by the oxygen atom linked to C_4 (imaginary frequency at 1389 cm^{-1}), lies at 16.0 kcal mol^{-1} (dashed line). In this species the C–H and H–O distances are 1.33 and 1.30 Å, while the O_{met}–C_{5PQQ} bond is 2.37 Å. The lower energy of TS2′a with respect to that of TS3a, corresponding to the breaking of C–H in mechanism A, can be explained by considering two factors. First of all, the negative charge of the cofactor, still present in this phase, makes the abstraction of the H^+ from the substrate CH by the C_4O carbonyl oxygen easier. Secondly, the instability of INT1a with respect to INT2a in the previous reaction path, due to a weaker bond between the calcium cation and a protonated aspartate, reduces the energetic cost to break the substrate

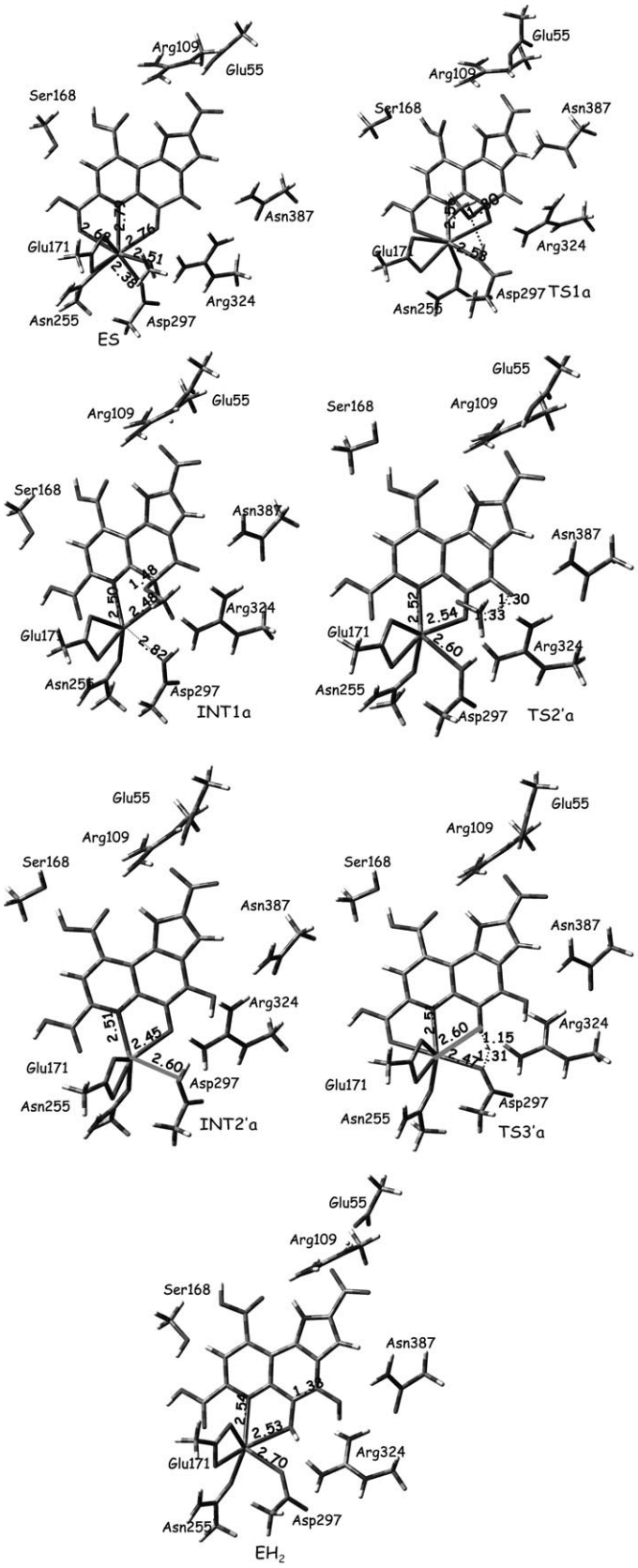

Figure 5. Optimized stationary points belonging to the revised addition–elimination path C.

CH bond. The barrier height (16.0 kcal mol^{-1}) may be now compatible with an enzymatic catalysis.

From TS2′a, an intermediate, INT2′a, in which the C_5O is negatively charged and the C_4O is protonated, is found 16.6 kcal mol^{-1} below the reference point, with the CH_2O product leaving the metallic centre.

Finally, through the transition-state TS3′a lying at 8.7 kcal mol^{-1} above INT2′a, responsible for the protonation of the PQQ C_5O oxygen atom, the reduction of the cofactor to the $PQQH_2$ is complete. The latter species is characterized by a network of hydrogen bonds especially involving the quinone molecule. Ca^{2+} results in being heptacoordinated to the oxygen atoms of Glu171 (2.41 and 2.38 Å), the Asn255 carbonyl oxygen (2.35 Å), the Asp297 oxygen (2.70 Å) and to the nitrogen and oxygen atoms of the cofactor (2.54, 2.57 and 2.53 Å, respectively).

Energetics in the protein environment: Results obtained in the gas phase (Figure 2) demonstrated that the mechanism by which methanol dehydrogenase enzyme oxidises methanol to formaldehyde should proceed through the addition–elimination process if one assumes that the C–H breaking of the alcohol occurs before the protonation of the cofactor. Only in this case, in fact, does the barrier that characterizes the rate determining step (16.0 kcal mol^{-1}) fall within the values compatible with an enzymatic reaction.

Our aim now is to verify whether the inclusion of the protein environment effects in the calculations confirms these findings.

The three PESs for both addition–elimination and hydride-transfer mechanisms, obtained applying the CPCM procedure[58,59] in which we have used a dielectric constant $\varepsilon = 4$[43–47] to describe the surrounding medium are reported in Figure 6.

Looking at path A (solid line, Figure 6a), the formation of the ES complex is less exothermic with respect to the gas phase (6.4 versus 12.9 kcal mol^{-1}). The TS1a, responsible for the nucleophilic addition of the alcoholic oxygen on the PQQ C_5 carbonyl carbon atom is located at 7.7 kcal mol^{-1} above the reference. The energy required to overcome this barrier is computed to be 14.1 kcal mol^{-1}. The INT1a species lies at 1.5 kcal mol^{-1} above the E+S reactants asymptote. The protonation of the cofactor through the TS2a requires an activation energy of 12.5 kcal mol^{-1}, and leads to the intermediate INT2a, lying at 12.4 kcal mol^{-1} below the reference. Finally, the energetic barrier to get through the TS3a transition state is computed to be 33.3 kcal mol^{-1}, which is practically the same as that computed in the gas phase (34.6 kcal mol^{-1}).

Dashed line (Figure 6a) represents the energetic profile for the case of the addition–elimination mechanism revised by us.

The cleavage of the CH bond through the TS2′a transition state shows an energetic barrier of 11.1 kcal mol^{-1}, as computed with respect to the INT1a intermediate. The energetic expense for the oxidation of methanol is reduced by the presence of the protein environment. The INT2′a species,

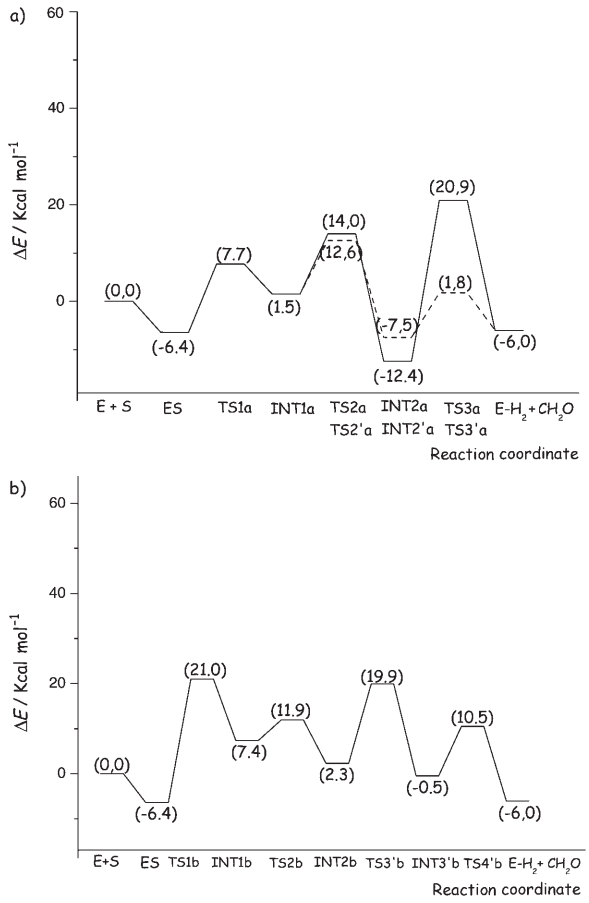

Figure 6. Potential-energy surface in the protein environment for (a) the addition–elimination mechanism and (b) the hydride-transfer mechanisms. Dielectric constant $\varepsilon = 4$.

leading to a C_4OH group in the cofactor, lies 7.5 kcal mol^{-1} below the reference. The final transition state (TS3′a) for the protonation of the C_5O oxygen in the PQQ by the Asp297 residue, shows an activation energy of 9.3 kcal mol^{-1}, very similar to that in the gas phase. EH_2 and CH_2O products are found 6.0 kcal mol^{-1} below the reactants.

In the case of the hydride-transfer mechanism (Figure 6b), the presence of the protein environment causes a certain stabilization of the TS1b species in the rate-determining step, but the activation energy of 27.4 kcal mol^{-1}, even if lowered by 4.9 kcal mol^{-1} with respect to that computed in the gas phase (32.3 kcal mol^{-1}), still remains too high for a biological catalytic process.

The conversion INT1b (7.4 kcal mol^{-1})→INT2b (2.3 kcal mol^{-1}) through TS2b (11.9 kcal mol^{-1}) entails an energetic cost of 4.5 kcal mol^{-1}.

We decided that it was meaningless to perform computations for the TS3b transition state in the protein medium, as its high gas-phase relative energy cannot undergo significant variations.

The energetic expense to complete the reduction of the cofactor to the $PQQH_2$ species is found in the protein environment to be higher than in the gas phase, owing to the TS3′b and TS4′b relative energies, 19.9 and 10.5 kcal mol^{-1}, respectively.

Conclusions

The catalysis of the PQQ-containing MDH enzyme was investigated at the density functional B3LYP level of theory, by employing a large reliable cluster (including up to 108 atoms) as model a system for the active site. The two controversial mechanisms proposed in literature, that is, the addition–elimination, which requires the nucleophilic addition of the methanol oxyanion on the PQQ cofactor followed by an intramolecular retroene reaction, and the hydride transfer, which involves the direct transfer of an H^- followed by an internal enolization process, were analysed in detail.

Both these mechanisms were proven to be incompatible with the kinetic requirements of the enzymatic processes. In fact, too high energy barriers (34.6 kcal mol^{-1} for addition–elimination, and 32.3 kcal mol^{-1} for the hydride-transfer mechanism) that exceed considerably the usual limits of 15–20 kcal mol^{-1}, were found in correspondence of the rate-determining step, that is, in both cases, the cleavage of the covalent C–H bond in the substrate.

A third mechanism, which we propose as an addition–elimination–protonation process in which the sequence of the steps involves the cleavage of the C–H bond in the substrate before the cofactor protonation by the Asp297 amino acid residue was found to be more reliable as the activation energy in the rate-determining step is 16.0 kcal mol^{-1} in the gas phase and 11.1 kcal mol^{-1} in the protein environment simulations.

The Asp297 residue acts as common acid–base catalyst by abstracting the proton from the substrate and then donating it, thus completely reducing the cofactor to the $PQQH_2$ species.

The role played by the Ca^{2+} cation consists in correctly orientating the cofactor and the substrate, and in polarizing the PQQ C_5=O carbonyl bond.

The addition–elimination–protonation mechanism proposed in this work can be regarded with confidence as the preferred reaction path followed by the PQQ-containing methanol dehydrogenase enzyme.

Acknowledgements

The University of Calabria and Regione Calabria (POR 2000/2006, misura 3.16, progetto PROSICA) is gratefully acknowledged.

[1] J. A. Duine, J. Frank, *Biochem. J.* **1980**, *187*, 221–226.
[2] V. L. Davidson, *Principles and applications of quinoproteins*, **1993**, Marcel Dekker, New York.
[3] W. S. McIntire, D. E. Wemmer, A. Chistoserdov, M. E. Lidstrom, *Science* **1991**, *252*, 817–824.
[4] S. M. Janes, D. Mu, D. Wemmer, A. J. Smith, S. Kaur, D. Maltby, A. L. Buringame, J. P. Klinman, *Science* **1990**, *248*, 981–987.

[5] J. P. Klinman, *Quinoproteins; Methods in Enzymology*, **1995**, Academic Press, New York.
[6] S. X. Wang, M. Mure, K. F. Medzihradszky, A. L. Burlingame, D. E. Brown, D. M. Dooley, A. J. Smith, H. M. Kagan, J. P. Klinman, *Science* **1996**, *273*, 1078–1084.
[7] C. Anthony, *Principles and Applications of Quinoproteins* (Ed.: V. L. Davidson) **1993**, Marcel Dekker, New York, pp. 17–45.
[8] C. Anthony, *Biochem. J.* **1996**, *320*, 697–711.
[9] C. Anthony, L. J. Zatman, *Biochem. J.* **1967**, *104*, 960–969.
[10] J. G. Hauge, *J. Biol. Chem.* **1964**, *239*, 3630–3639.
[11] Z. X. Xia, W. W. Dai, J. P. Xiong, Z. P. Hao, V. L. Davidson, S. White, F. S. Mathews, *J. Biol. Chem.* **1992**, *267*, 22289–22297.
[12] S. White, G. Boyd, F. S. Mathews, Z. X. Xia, W. W. Dai, Y. F. Zhang, V. L. Davidson, *Biochemistry* **1993**, *32*, 12955–12958.
[13] C. Anthony, M. Ghosh, C. C. F. Blake, *Biochem. J.* **1994**, *304*, 665–674.
[14] M. Ghosh, C. Anthony, K. Harlos, M. G. Goodwin, C. C. F. Blake, *Structure* **1995**, *3*, 177–187.
[15] Z. Xia, W. Dai, Y. Zhang, S. A. White, G. D. Boyd, F. S. Mathews, *J. Mol. Biol.* **1996**, *259*, 480–501.
[16] K. Matsushita, K. Takahashi, O. Adachi, *Biochemistry* **1993**, *32*, 5576–5582.
[17] J. J. Meulenberg, E. Sellink, N. H. Riegman, P. W. Postma, *Mol. Gen. Genet.* **1992**, *232*, 284–294.
[18] O. Adachi, K. Matsushita, E. Shinagawa, M. Ameyama, *Agric. Biol. Chem.* **1990**, *54*, 2833–2837.
[19] J. W. Richardson, C. Anthony, *Biochem. J.* **1992**, *287*, 709–715.
[20] C. C. F. Blake, M. Ghosh, K. Harlos, A. Avezoux, C. Anthony, *Nat. Struct. Biol.* **1994**, *1*, 102–195.
[21] Z. Xia, W. Dai, Y. Zhang, S. A. White, G. D. Boyd, F. S. Mathews, *J. Mol. Biol.* **1996**, *259*, 480–501.
[22] J. J. Frank, M. Dijkstra, J. A. Duine, C. Balny, *Eur. J. Biochem.* **1988**, *174*, 331–338.
[23] J. J. Frank, S. H. van Krimpen, P. E. Verwiel, J. A. Jongejan, A. C. Malder, J. A. Duine, *Eur. J. Biochem.* **1989**, *184*, 187–195.
[24] A. J. Olisthoorn, J. A. Duine, *Biochemistry* **1998**, *37*, 13854–13861.
[25] Y. J. Zheng, T. C. Bruice, *Proc. Natl. Acad. Sci. USA* **1997**, *94*, 11881–11886.
[26] A. Oubrie, H. J. Rozeboom, K. H. Kalk, A. J. J. Olsthoom, J. A. Duine, B. W. Dijkstra, *EMBO J.* **1999**, *18*, 5187–5194.
[27] Z. X. Xia, Y.-N. He, W. W. Dai, Y. F. Zhang, S. A. White, G. D. Boyd, F. S. Mathews, *Biochemistry* **1999**, *38*, 1214–1220.
[28] Y.-J. Zheng, Z.-X. Xia, Z.-W. Chen, F. S. Mathews, T. C. Bruice, *Proc. Natl. Acad. Sci. USA* **2001**, *98*, 432–434.
[29] S. Y. Reddy, T. C. Bruice, *J. Am. Chem. Soc.* **2003**, *125*, 8141–8150.
[30] C. W. M. Kay, B. Mennenga, H. Gorisch, R. Bittl, *J. Am. Chem. Soc.* **2005**, *127*, 7974–7975.
[31] Gaussian 03, Revision C.02, M. J. Frisch, G. W. Trucks, H. B. Schlegel, G. E. Scuseria, M. A. Robb, J. R. Cheeseman, J. A. Montgomery, Jr., T. Vreven, K. N. Kudin, J. C. Burant, J. M. Millam, S. S. Iyengar, J. Tomasi, V. Barone, B. Mennucci, M. Cossi, G. Scalmani, N. Rega, G. A. Petersson, H. Nakatsuji, M. Hada, M. Ehara, K. Toyota, R. Fukuda, J. Hasegawa, M. Ishida, T. Nakajima, Y. Honda, O. Kitao, H. Nakai, M. Klene, X. Li, J. E. Knox, H. P. Hratchian, J. B. Cross, V. Bakken, C. Adamo, J. Jaramillo, R. Gomperts, R. E. Stratmann, O. Yazyev, A. J. Austin, R. Cammi, C. Pomelli, J. W. Ochterski, P. Y. Ayala, K. Morokuma, G. A. Voth, P. Salvador, J. J. Dannenberg, V. G. Zakrzewski, S. Dapprich, A. D. Daniels, M. C. Strain, O. Farkas, D. K. Malick, A. D. Rabuck, K. Raghavachari, J. B. Foresman, J. V. Ortiz, Q. Cui, A. G. Baboul, S. Clifford, J. Cioslowski, B. B. Stefanov, G. Liu, A. Liashenko, P. Piskorz, I. Komaromi, R. L. Martin, D. J. Fox, T. Keith, M. A. Al-Laham, C. Y. Peng, A. Nanayakkara, M. Challacombe, P. M. W. Gill, B. Johnson, W. Chen, M. W. Wong, C. Gonzalez, J. A. Pople, Gaussian, Inc., Wallingford CT, **2004**.
[32] A. D. J. Becke, *Chem. Phys.* **1993**, *98*, 5648–5652.
[33] C. Lee, W. Yang, R. G. Parr, *Phys. Rev. B* **1988**, *37*, 785–789.
[34] A. D. Becke, *J. Chem. Phys.* **1993**, *98*, 1372.
[35] A. D. Becke, *Phys. Rev. B* **1988**, *38*, 3098.
[36] M. B. Hall, C. E. Webster, *J. Am. Chem. Soc.* **2001**, *123*, 5820–5821.
[37] R. A. Friesner, M. D. Beachy, *Curr. Opin. Struct. Biol.* **1998**, *8*, 257–262.
[38] P. E. M. Siegbahn, M. R. A. Blomberg, *Annu. Rev. Phys. Chem.* **1999**, *50*, 221–249.
[39] F. Bernardi, A. Bottoni, R. Casadio, P. Fariselli, A. Rigo, *Int. J. Quantum Chem.* **1996**, *58*, 109–119.
[40] F. Bernardi, A. Bottoni, R. Casadio, P. Fariselli, A. Rigo, *Inorg. Chem.* **1996**, *35*, 5207–5212.
[41] M. Flock, K. Pieloot, *J. Phys. Chem. A* **1999**, *103*, 95–102.
[42] T. Lind, P. E. M. Siegbahn, R. H. Crabtree, *J. Phys. Chem. B* **1999**, *103*, 1193–1202.
[43] P. E. M. Siegbahn, M. R. A. Blomberg, *Chem. Rev.* **2000**, *100*, 421–437.
[44] L. Noodleman, T. Lovell, W. G. Han, J. Li, F. Himo, *Chem. Rev.* **2004**, *104*, 459–508.
[45] M. Leopoldini, N. Russo, M. Toscano, M. Dulak, A. T. Wesoloski, *Chem. Eur. J.* **2006**, *12*, 2532–2541.
[46] M. Leopoldini, N. Russo, M. Toscano, *J. Phys. Chem. B* **2006**, *110*, 1063–1072.
[47] T. Marino, N. Russo, M. Toscano, *J. Am. Chem. Soc.* **2005**, *127*, 4242–4253.
[48] R. Ditchfield, W. J. Hehre, J. A. Pople, *J. Chem. Phys.* **1971**, *54*, 724–728.
[49] W. J. Hehre, R. Ditchfield, J. A. Pople, *J. Chem. Phys.* **1972**, *56*, 2257–2261.
[50] P. C. Hariharan, J. A. Pople, *Mol. Phys.* **1974**, *27*, 209–214.
[51] M. S. Gordon, *Chem. Phys. Lett.* **1980**, *76*, 163–168.
[52] P. J. Hay, W. R. Wadt, *J. Chem. Phys.* **1985**, *82*, 270–283; P. J. Hay, W. R. Wadt, *J. Chem. Phys.* **1985**, *82*, 284–298; P. J. Hay, W. R. Wadt, *J. Chem. Phys.* **1985**, *82*, 299–310.
[53] C. Gonzalez, H. B. Schlegel, *J. Chem. Phys.* **1989**, *90*, 2154.
[54] C. Gonzalez, H. B. Schlegel, *J. Phys. Chem.* **1990**, *94*, 5523.
[55] S. Miertus, E. Scrocco, J. Tomasi, *Chem. Phys.* **1981**, *55*, 117–129.
[56] S. Miertus, J. Tomasi, *Chem. Phys.* **1982**, *65*, 239–245.
[57] M. Cossi, V. Barone, R. Commi, J. Tomasi, *Chem. Phys. Lett.* **1996**, *255*, 327.
[58] V. Barone, M. Cossi, *J. Phys. Chem. A* **1998**, *102*, 1995–2001.
[59] M. Cossi, N. Rega, G. Scalmani, V. Barone, *J. Comput. Chem.* **2003**, *24*, 669–681.
[60] V. Barone, M. Cossi, B. Menucci, J. Tomasi, *J. Chem. Phys.* **1997**, *107*, 3210–3221.
[61] E. D. Glendening, A. E. Reed, J. E. Carpenter, F. Weinhold, *NBO*, Version 3.1.

Received: August 2, 2006
Published online: December 6, 2006

